

# Exposure to urban particulate matter (UPM) impairs mitochondrial dynamics in BV2 cells, triggering a mitochondrial biogenesis response

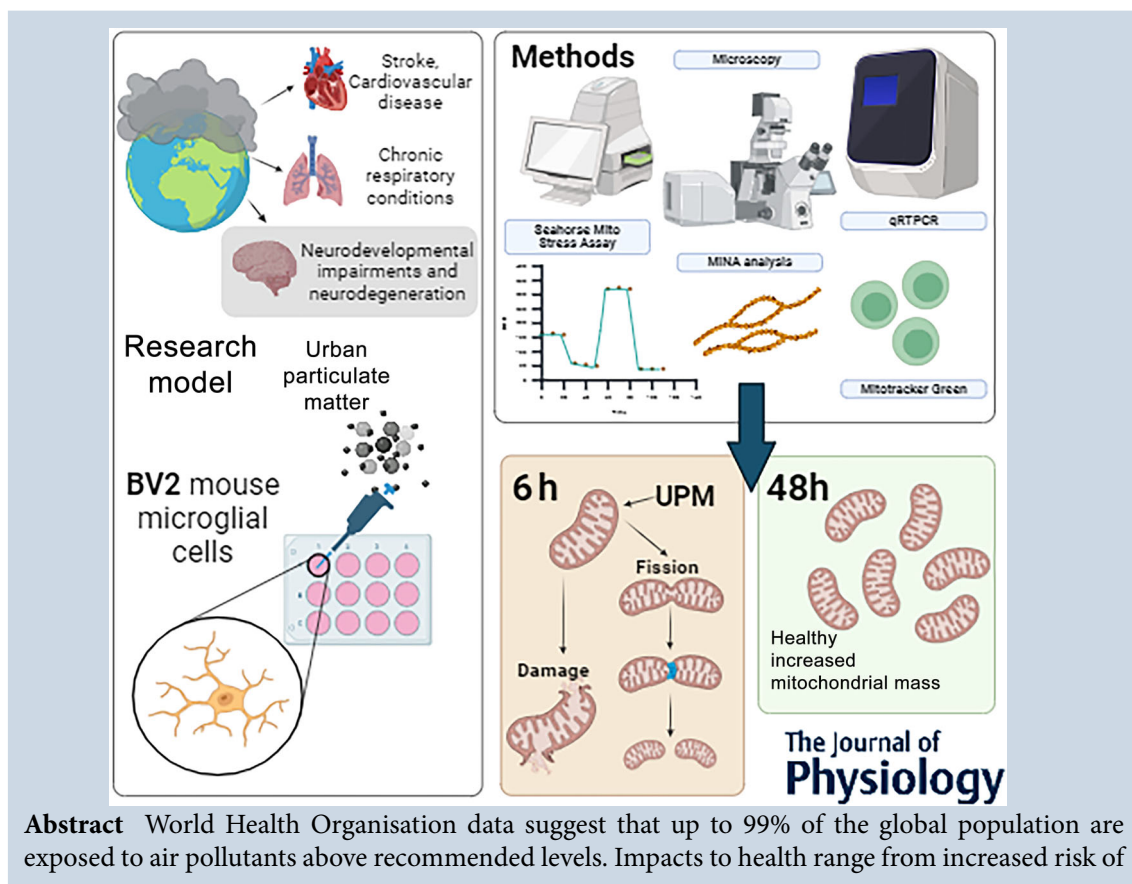
Rebecca H. Morris<sup>1</sup>, Serena J. Counsell<sup>2</sup>, Imelda M. McGonnell<sup>1</sup> and Claire Thornton<sup>1,2</sup> 

<sup>1</sup>Department of Comparative Biomedical Sciences, Royal Veterinary College, London, UK

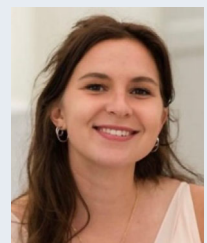
<sup>2</sup>Centre for the Developing Brain, School of Biomedical Engineering & Imaging Sciences, King's College London, London, UK

Handling Editors: Laura Bennet & Christopher Lear

The peer review history is available in the Supporting Information section of this article (<https://doi.org/10.1113/JP285978#support-information-section>).



**Rebecca H. Morris** earned a BSc in Pharmacology and Molecular Genetics, and a Masters in Neuropharmacology, fuelled by a profound interest in neurodegenerative diseases. Understanding the intricacies of the brain, its function, and vulnerability during neurodegeneration and neurodevelopment has been a driving force. In her PhD, she conducted *in vitro*, *in vivo* and sequencing studies to unravel the impact of air pollution on the developing brain, focusing on cellular metabolism. She is now at a biotechnology firm, contributing to drug discovery innovation, utilising the power of knowledge graphs and artificial intelligence to better understand disease processes and how to target them.



stroke and cardiovascular disease to chronic respiratory conditions, and air pollution may contribute to over 7 million premature deaths a year. Additionally, mounting evidence suggests that *in utero* or early life exposure to particulate matter (PM) in ambient air pollution increases the risk of neurodevelopmental impairment with obvious lifelong consequences. Identifying brain-specific cellular targets of PM is vital for determining its long-term consequences. We previously established that microglial-like BV2 cells were particularly sensitive to urban (U)PM-induced damage including reactive oxygen species production, which was abrogated by a mitochondrially targeted antioxidant. Here we extend those studies to find that UPM treatment causes a rapid impairment of mitochondrial function and increased mitochondrial fragmentation. However, there is a subsequent restoration of mitochondrial and therefore cell health occurring concomitantly with upregulated measures of mitochondrial biogenesis and mitochondrial load. Our data highlight that protecting mitochondrial function may represent a valuable mechanism to offset the effects of UPM exposure in the neonatal brain.

(Received 14 November 2023; accepted after revision 6 May 2024; first published online 25 May 2024)

**Corresponding author** C. Thornton: Department of Comparative Biomedical Sciences, Royal Veterinary College, London, UK. Email: cthornton@rvc.ac.uk

**Abstract figure legend** Air pollution affects most of the planet's population. Unsurprisingly, pollution-related chronic respiratory conditions and cardiovascular disease are becoming more prevalent, but emerging data suggest that airborne particulate matter exposure also impacts neurodevelopment and may play a role in neurodegeneration. In this study, we examine the effects of urban particulate matter (UPM) exposure on BV2 microglial-like cells, evaluating mitochondrial structure and function. We find that mitochondrial membrane potential and cellular bioenergetics are rapidly impaired after UPM treatment. Subsequently there is an increase in markers of mitochondrial biogenesis, which may constitute a cellular mitigation strategy. Protecting mitochondrial function may be crucial in ameliorating the effects of airborne pollution exposure particularly in the developing brain where consequences are lifelong.

### Key points

- Air pollution represents a growing risk to long-term health especially in early life, and the CNS is emerging a target for airborne particulate matter (PM).
- We previously showed that microglial-like BV2 cells were vulnerable to urban (U)PM exposure, which impaired cell survival and promoted reactive oxygen species production.
- Here we find that, following UPM exposure, BV2 mitochondrial membrane potential is rapidly reduced, concomitant with decreased cellular bioenergetics and increased mitochondrial fission.
- However, markers of mitochondrial biogenesis and mitochondrial mass are subsequently induced, which may represent a cellular mitigation strategy.
- As mitochondria are more vulnerable in the developing brain, exposure to air pollution may represent a greater risk to lifelong health in this cohort; conversely, promoting mitochondrial integrity may offset these risks.

## Introduction

Air pollution, particularly particulate matter (PM), is a prevalent public health concern with increasing evidence linking it to morbidity and mortality (Chen & Hoek, 2020; Orellano et al., 2020). The World Health Organisation (WHO) suggests that 99% of the population are habitually exposed to higher than recommended levels of PM originating from various sources such as transport, domestic fuel burning, industry, and human and natural sources (Karagulian et al., 2015). Emerging

data suggesting that even exposure to low levels of PM can be injurious (Pérez Velasco & Jarosińska, 2022; Whaley et al., 2021) prompted the WHO to reappraise and reduce their original guidelines (Supplementary Table 1; WHO, 2021). Inhalation is the main route of PM exposure, where smaller particles (PM<sub>2.5</sub>) can infiltrate the lungs (Thangavel et al., 2022), associated with an increased risk of cardiovascular and respiratory diseases (Arias-Perez et al., 2020; Kim et al., 2018; Miller, 2020). However, there is growing evidence suggesting that PM can have adverse effects on the CNS (Kim, Kim et al., 2020; You

**Table 1. Primers used in the study**

Gene (accession)	Name	Primer
<i>Tfam</i> (NM_009360)	Transcription factor A, mitochondrial	Mm00447485_m1
<i>Ppargc1α</i> (NM_008904)	PPARG coactivator 1 alpha	Mm00447183_m1
<i>Drp1</i> (NM_001025947)	Dynamic-related protein 1	Mm01342903_m1
<i>Mff</i> (NM_029409)	Mitochondrial fission factor	Mm01273401_m1
<i>Fis1</i> (NM_001163243)	Fission, mitochondrial 1	Mm00481580_m1
<i>Gapdh</i> (NM_008084)	Glyceraldehyde 3-phosphate dehydrogenase	Mm99999915_g1

et al., 2022), contributing to long-term detrimental effects on brain health (Costa et al., 2020; Morris et al., 2021). Furthermore, exposure to PM *in utero* increases neurotoxicity and neuroinflammation in rodent offspring models, and epidemiological studies have found an increased risk of autism spectrum disorder especially in males following maternal exposure to PM (Bilbo et al., 2018; Bolton et al., 2013; Rahman et al., 2022).

Microglia are the resident immune cells of the brain and, in addition to their known role in acute defence against infection, contribute to brain development through synaptic pruning and maintenance of brain homeostasis (Mallard et al., 2019). However, aberrant/persistent microglial activation is a hallmark of a number of neonatal pathologies. In the developing brain, activation of microglia is observed following encephalopathy of prematurity as well as in the sequelae of birth asphyxia and neonatal stroke (Fleiss et al., 2021; Mallard et al., 2019). The subsequent neuroinflammatory response contributes to common outcomes for these infants such as neurological, behavioural and motor impairments, which have lifelong consequences (Fleiss et al., 2021).

Mitochondria reside in all brain cell types and, notably, brain mitochondria are some of the most long-lived in the body (20–30 days, compared with 10 days for the liver) therefore requiring significant quality control (Krishna et al., 2021; Menzies & Gold, 1971; Navarro & Boveris, 2004; Stauch et al., 2023). Energy utilisation by the brain is disproportionately high given its size and there is a significant increase in metabolic demand during early years of brain development (Kuzawa et al., 2014). Mitochondria are known for their ability to generate ATP through oxidative phosphorylation, as well as for calcium buffering, cell death pathways and steroid hormone synthesis. In the brain, healthy mitochondrial function supports neurite outgrowth, neurotransmitter release, neurogenesis, neuronal plasticity and synaptic function, and mediates the inflammatory response (Culmsee et al., 2018; Misgeld & Schwarz, 2017). However, the immature brain is more vulnerable to neurotoxicity, especially due to high levels of extracellular iron and decreased anti-

oxidants (Blomgren & Hagberg, 2006); repeated studies have identified impaired mitochondrial dysfunction in preclinical models of neonatal brain injury (Hagberg et al., 2014; Jones & Thornton, 2022).

Mitochondria in the CNS are increasingly being investigated as targets for air pollution (Chew et al., 2020). PM-bound metals can impair mitochondrial structure, disturb mitochondrial membrane potential and calcium buffering capabilities, and induce intracellular mitochondrial reactive oxygen species (mtROS) production and pro-apoptotic factors into the cytoplasm, which are known to trigger cellular stress pathways (Pardo et al., 2020). *In vivo*, mitochondrial matrix swelling was observed in hippocampal cells from the offspring of mice exposed to PM<sub>2.5</sub> during gestation (Zheng et al., 2018). Similarly, in rodents exposed to PM postnatally, there was an increase in neuroinflammation with a concomitant suppression of mitochondrial gene expression in the hippocampus, and a learning and memory impairment (Li et al., 2018; Li et al., 2020).

We previously showed that exposure to urban (U)PM induces neurotoxicity in microglial-like BV2 cells, with augmented neuroinflammation and oxidative stress (Morris et al., 2022). Pretreatment with a mitochondrially targeted antioxidant rescued UPM-induced cell death and reduced mtROS production to control levels. Moreover, UPM exposure increased apoptosis, suggesting rupture of the cristae and damage to mitochondria. Mitochondrial dysfunction may be a target for the pathological mechanisms underpinning brain impairment following microglial UPM exposure. Here we extend these findings to examine the effect of UPM exposure directly on mitochondria dynamics and associated cellular bioenergetics in microglial-like BV2 cells.

## Materials and methods

### BV2 cell culture and UPM treatment

The female neonatal mouse microglia BV2 cell line was provided by Professor R. Donato (University of Perugia, Italy), cultured as described previously (Morris

et al., 2022) and used between passage (P)2 and P22. For treatments, BV2 cells were transferred to medium containing 5% fetal bovine serum (FBS). Stock solutions were prepared by suspending UPM (Sigma, St Louis, MO, USA, #NIST1648A, certified reference material; Wang et al., 2020) in Dulbecco's modified Eagle's medium (DMEM) growth medium and working solutions prepared by sonication as described previously (Morris et al., 2022).

### Detection of mitochondrial membrane potential

Changes in mitochondrial membrane potential were analysed by incubation with tetramethylrhodamine (TMRM, 200 nM, ThermoFisher, Waltham, MA, USA). Following incubation (30 min, 37°C/5% CO<sub>2</sub>), cells were rinsed with phosphate-buffered saline (PBS) and imaged (EVOS M5000). Corrected total cellular fluorescence (CTCF; Bora et al., 2021) was quantified in ImageJ using the formula:

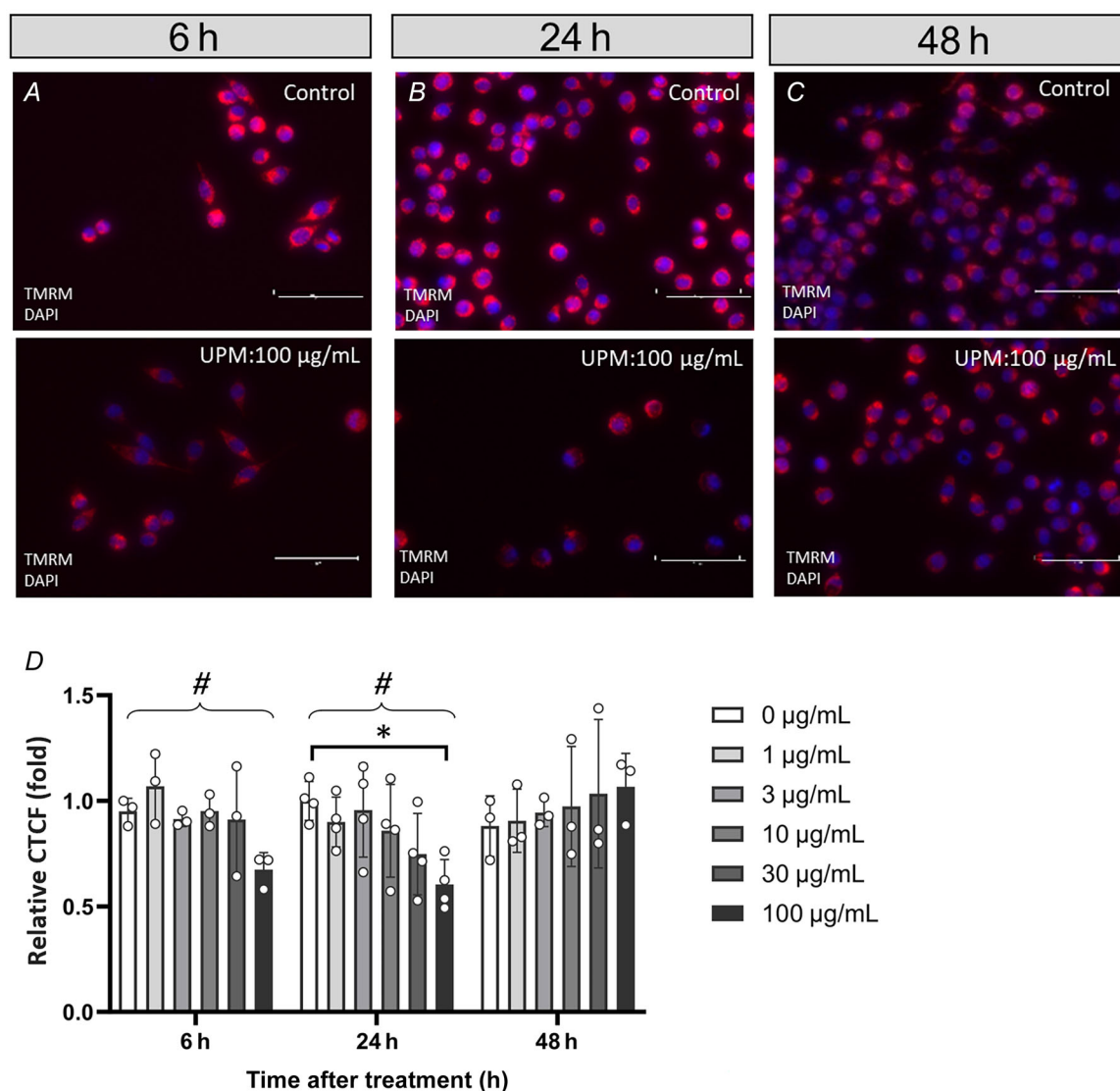


**Figure 1. UPM exposure dissipates mitochondrial membrane potential**

BV2 cells were exposed to UPM (0–100 µg/mL) and then labelled with TMRM. At 6 h (A, D) and 24 h (B, D) following UPM treatment, a decrease in TMRM fluorescence was observed (linear trend at 6 h:  $^{\#}P = 0.0181$ , slope =  $-0.0519$ ; 24 h:  $^{\#}P = 0.0378$ , slope =  $-0.0202$ , 0 µg/mL vs. 100 µg/mL,  $^{*}P = 0.0297$ ) At 48 h (C, D), no differences were observed in relative TMRM fluorescence (48 h: 0 µg/mL vs. 100 µg/mL,  $P = 0.843$ ). Scale bar represents 100 µm. Data were analysed by a one-way ANOVA followed by Sidak's *post hoc* test. Biological replicates ( $N = 3$ –4) are means of three technical replicates. Data are expressed as mean  $\pm$  SD. CTCF: corrected total cell fluorescence. [Colour figure can be viewed at [wileyonlinelibrary.com](https://onlinelibrary.wiley.com/terms-and-conditions)]



CTCF = integrated density – (area of selected cell  
× mean fluorescence of background reading)

### Mitochondrial respiration measurement (Seahorse)

The Seahorse XF cell mitochondria stress test kit (Agilent, Santa Clara, CA, USA) was used to assess mitochondrial function in control and 100 µg/mL UPM-treated BV2 cells. Cells were seeded (6000 per well) onto an XF96 plate and treated with UPM as above. Oxygen consumption rates (OCRs) were measured using the mitochondrial stress test assay in XF DMEM media, 1 mM pyruvate and 2 mM L-glutamine. Measurements were taken under basal conditions and following injections of oligomycin (2 mM), FCCP (carbonyl cyanide-p-trifluoromethoxyphenylhydrazone, 1 mM), rotenone and antimycin A (0.5 mM) with the Seahorse XF96 HS Mini Analyser. In addition to the raw traces, data are presented as fold change compared with the mean of the control values for comparison.

### Confocal microscopy and mitochondrial network analyses

BV2 cells were seeded ( $8 \times 10^5$  per well; 12-well plate) onto sterile glass coverslips and after 24 h cells, once they had adhered, were treated with UPM (0–100 µg/mL; 0–48 h). As per the detection of mitochondrial mass, similarly BV2 cells were incubated with 100 nM Mitotracker orange (30 min, 37°C/5% CO<sub>2</sub> ThermoFisher) before being washed with PBS. Cells were fixed with 4% (w/v) paraformaldehyde in PBS (20 min, room temperature) and washed thoroughly with PBS before mounting onto slides using Prolong Diamond antifade mounting medium with DAPI (ThermoFisher). Images were obtained on the Leica SP8 confocal microscope with a 63× oil objective. Images were analysed in Image J using the mitochondrial network analysis (MiNA) macro, allowing for semi-automated analysis of mitochondrial networks in mammalian cells (Valente et al., 2017).

### Gene expression analysis

RNA from BV2 cells was prepared and analysed by one-step quantitative (q)RT-PCR (Taqman RNA-to-Ct 1-step kit, ThermoFisher) as described previously (Morris et al., 2022) using prevalidated TaqMan primers (ThermoFisher; Table 1). Relative gene expression was determined by normalisation to both GAPDH and experimental controls using the Delta Ct method (Livak & Schmittgen, 2001).

### Western blot analyses

Cells were lysed in HBA lysis buffer, 30–50 µg was analysed by 4–12% SDS-PAGE and western blot as described previously (Morris et al., 2022). REVERT 700 Total Protein Stain (TPS, LiCOR Bioscience, Lincoln, NE, USA) was used according to the manufacturer's instructions to quantify total protein. Proteins were detected using primary antibodies anti-DRP1 (Abcam, #ab156951, 1:1000, Cambridge, MA, USA) and anti-DRP1pSer616 (Cell Signaling, #3455, Danvers, MA, USA) and appropriate secondary IRDye 600CW or IRDye800 antibodies (LiCOR Bioscience, 1:10,000).

### Detection of mitochondrial mass

Changes in mitochondrial mass following UPM exposure were determined using mitotracker green staining (100 nM, ThermoFisher). Following incubation (30 min, 37°C/5% CO<sub>2</sub>), cells were washed with PBS, medium was replaced and plates were imaged (EVOS M5000). CTCF was calculated as above.

### Statistics

Sample size (*N*) indicates biological replicates which, for cell culture studies, represents experiments at different passages. Technical repeats (two to three) were carried out within each biological replicate. Statistical analysis was conducted using Prism Software (v9, GraphPad, La Jolla, CA, USA). Data were evaluated for normality using the Shapiro–Wilk test and then assessed using two-way or one-way ANOVA, followed by appropriate *post hoc* tests or for linear trend (indicated with curly brackets on graphs), stated in the text. For single conditions (e.g. Fig. 3), data were analysed by an unpaired, two tailed *t* test. Image analysis was performed using Fiji software (ImageJ) with suitable plug-in macros when required.

### Results

#### Exposure to UPM rapidly reduces mitochondrial membrane potential

We previously observed that mtROS levels were significantly increased following UPM (100 µg/mL) exposure in BV2 cells, and that this ROS accumulation could be prevented by preincubation with a mitochondrially targeted antioxidant, Mitotempo (Morris et al., 2022). As this ROS was probably mitochondrial in origin, we measured mitochondrial membrane potential in BV2 cells at time points following UPM exposure (0–100 µg/mL). At 6 and 24 h (Fig. 1A, B and D) there was a significant decreasing trend in TMRM fluorescence (6 h: *P* = 0.0181, 24 h *P* = 0.0378), most noticeably at

the highest UPM dose (24 h: 0  $\mu\text{g/mL}$  vs. 100  $\mu\text{g/mL}$ ,  $P = 0.0297$ ) indicating a dissipation of mitochondrial membrane potential. However, at 48 h following UPM treatment, there was no significant trend ( $P = 0.2196$ ) or differences in TMRM fluorescence observed (Fig. 1C and D), suggesting that 48 h after UPM exposure, any decreases in mitochondrial membrane potential and subsequent loss in mitochondrial integrity are ameliorated.

### UPM exposure alters cellular bioenergetics

To evaluate the functional consequence of UPM-mediated dissipation of mitochondrial membrane potential, we performed bioenergetic profiling of BV2 cells exposed to UPM (100  $\mu\text{g/mL}$ ) by measuring OCR (Fig. 2A). At 6 h, there was a decrease in basal respiration (Fig. 2B) accompanied by a significant decrease in ATP production (Fig. 2C,  $P = 0.0361$ ). Surprisingly, at 24 h, measurements of key parameters such as basal respiration and ATP production were the inverse of those observed at 6 h

(Fig. 2B and C). There was no significant difference observed in proton leak (Fig. 2D), but there was a significant increase in maximal respiration at 24 h compared with 6 and 48 h UPM-treated cells (Fig. 2D,  $P = 0.0064$ ) and with untreated cells at 24 h (Fig. 2D,  $P = 0.0044$ ). These data suggest that after 24 h, UPM exposure results in an augmented rate of metabolism to support normal cell functioning. At 48 h after UPM exposure, no significant differences from control were observed for any of the parameters measured (Fig. 2B–E).

### UPM exposure alters mitochondrial morphology

Given the surprising rebound in mitochondrial function seen at 24 h following UPM exposure, we evaluated whether the UPM-mediated changes in bioenergetics were accompanied by alterations in mitochondrial dynamics. Mitochondria alter their morphology through fission and fusion cycles to balance energy production, mitochondrial quality control and biogenesis. The

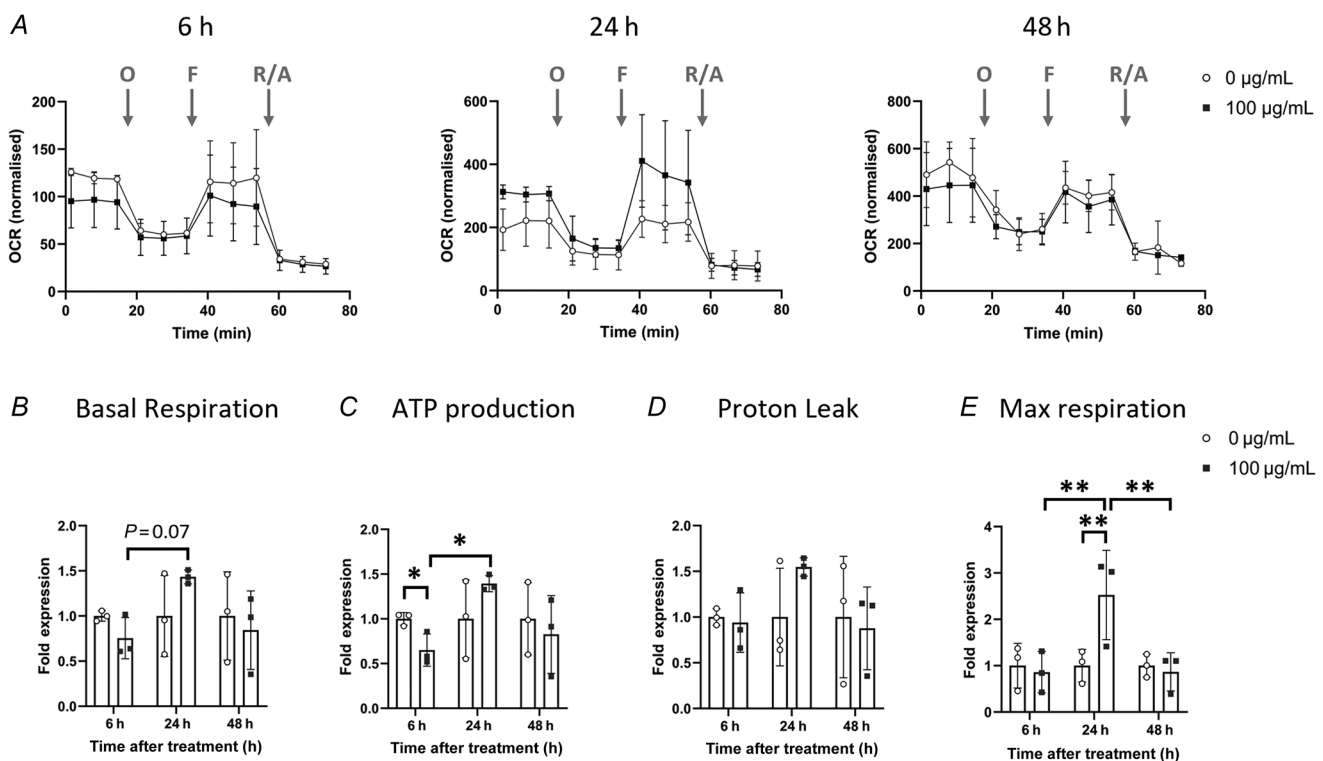


**Figure 2. UPM exposure alters OCR values in a time- and concentration-dependent manner**

A, Mito stress test analysis was performed on BV2 cells at 6, 24 and 48 h following UPM exposure (100  $\mu\text{g/mL}$ ). Oxygen consumption rate (OCR) was measured at a basal rate and following the injections of oligomycin (O, 2 mM), FCCP (F, 1 mM) and rotenone/antimycin A (R/A, 0.5 mM). Data were normalised to cell number. B–E, bioenergetic metrics are altered between 6 and 24 h, resolving by 48 h. Data are expressed as fold change relative to the average control value at the indicated timepoints. B, basal respiration: 6 h 100  $\mu\text{g/mL}$  vs. 24 h 100  $\mu\text{g/mL}$ ,  $P = 0.0731$ . C, ATP production: 6 h 0  $\mu\text{g/mL}$  vs. 100  $\mu\text{g/mL}$ ,  $*P = 0.0361$ ; 6 h 100  $\mu\text{g/mL}$  vs. 24 h 100  $\mu\text{g/mL}$ ,  $*P = 0.0329$ . D, proton leak. E, maximum respiration: 6 h 100  $\mu\text{g/mL}$  vs. 24 h 100  $\mu\text{g/mL}$ ,  $**P = 0.0064$ ; 24 h 0  $\mu\text{g/mL}$  vs. 100  $\mu\text{g/mL}$ ,  $**P = 0.0044$ ; 24 h 100  $\mu\text{g/mL}$  vs. 48 h 100  $\mu\text{g/mL}$ ,  $**P = 0.0066$ . Data were analysed by two-way ANOVA followed by Tukey *post hoc* test ( $N = 3$ , with three technical replicates) and expressed as mean  $\pm$  SD.

equilibrium between fission and fusion is crucial for normal mitochondrial functioning (Kyriakoudi et al., 2021). BV2 cells were treated with UPM and stained with mitotracker orange before fixing, imaging and evaluating using MiNA software (Valente et al., 2017)). There were clear and rapid changes in mitochondrial morphology at 6 h (Fig. 3A) where the number of individual mitochondria increased significantly ( $P = 0.0177$ ), accompanied by a loss of reticular complexity [increased networks ( $P = 0.0449$ ) but reduced branching ( $P = 0.0132$ ), Fig. 3B–E). In contrast, no differences in morphometrics were observed at 24 h following UPM treatment (Fig. 3A, F–I).

As induction of mitochondrial fission was implicated from these data, further investigation of the mitochondrial fission regulator dynamin-related protein (DRP)1 was performed. Increases in *Drp1* gene expression which reached almost 4-fold were triggered 6 h after UPM exposure, and dissipated by 24 h (Fig. 4A,  $P = 0.0162$ ). Increased *Mff* expression was also apparent (Fig. 4B,  $P = 0.0181_{[\text{time}]}$ ,  $P = 0.0284_{[\text{conc}]}$ ) specifically at 30  $\mu\text{g/mL}$  UPM ( $P = 0.0447$ ). However, regardless of concentration, UPM exposure had no effect on the gene expression of another regulator of mitochondrial fission, *Fis1* (Fig. 4C).

Interestingly, DRP1 protein expression decreased linearly with respect to concentration at 6 h after treatment (Fig. 4D and E,  $P = 0.0353$ ) but was restored by 24 h (Fig. 4D and F). S616 DRP1 phosphorylation was maintained throughout, leading to an overall increase in the ratio of phospho:total DRP1 at 6 h (Fig. 4F,  $P = 0.0370$ ), suggesting a drive towards mitochondrial fission.

### Exposure to UPM increases mitochondrial mass after 24 h

A recent study suggested that the fate of fissioned mitochondria depended on whether the fission event was midzone (driven by MFF) or peripheral (driven by FIS1; Kleele et al., 2021). Midzone fission feeds the process of mitochondrial biogenesis, whereas asymmetric fission facilitates mitophagy of the smaller, damaged mitochondria. Given our gene expression data (Fig. 4) and the rebound of mitochondrial function seen at 24 h after UPM exposure (Fig. 2), we investigated whether mitochondrial biogenesis was upregulated. We found increased expression of two gatekeepers of mitochondrial biogenesis, *Tfam* and *Ppargc1 $\alpha$*  (PGC1 $\alpha$ ) at 6 and 24 h after UPM exposure (Fig. 5A and B). Significant linear trends in expression were observed, correlating with increased concentrations of UPM, in both *Tfam* and *Ppargc1 $\alpha$*  at 24 h [Fig. 5A, *Tfam* (24 h):  $P = 0.0008$ , Fig. 5B, *Ppargc1 $\alpha$*  (24 h):  $P = 0.0322$ ]. Staining of cells with mitotracker green (independent of mitochondrial

membrane potential) revealed no difference at 6 h after UPM treatment (Fig. 5C and F). There were, however, significant increases in mitotracker fluorescence apparent at 24 h (Fig. 5D and F,  $P < 0.0001$  for linear trend) and these were maintained at 48 h (Fig. 5E and F,  $P = 0.0003$  for linear trend).

## Discussion

With mounting evidence suggesting the brain as a target for PM and the role of mitochondrial function in PM-induced neurotoxicity (Chew et al., 2020; Morris et al., 2021), there is an urgent, unmet need to better understand how UPM exposure affects mitochondrial health and dynamics. Following on from our previous work where we identified increased mtROS in BV2 microglial-like cells following UPM exposure (Morris et al., 2022), here we took an in-depth approach to evaluate mitochondrial health following treatment with UPM. UPM exposure rapidly impaired mitochondrial membrane potential and increased mitochondrial fission in BV2 cells within 6 h. However, the cellular response to this insult resulted in increased mitochondrial biogenesis signalling and a restoration of mitochondrial bioenergetics.

Microglial-like BV2 cells (Bai et al., 2019; Chen et al., 2018; Kim, Shin et al., 2020; Sama et al., 2007) and primary microglia (Block et al., 2004; Levesque et al., 2011) have been previously studied in the context of air pollution and show significant pathological responses to a variety of particulate matter (e.g. PM<sub>2.5</sub>, PM<sub>10</sub>, diesel exhaust particles). These studies identified significant PM-mediated pathological responses including cell death, proinflammatory gene expression and ROS production, as well as inducing bystander death in co-cultured neurons. In our current and previous studies using BV2 cells, we identified both rapid/direct and delayed/indirect responses to UPM treatment including mitochondrial ROS production, and mitochondrial impairment followed by increases in mitochondrial mass within the cell. We have also observed apparent UPM accumulation within BV2 cells (R. Morris, unpublished observation) suggesting that phagocytic cells such as microglia may have an extra vulnerability as engulfment may result in focal long-lasting high concentrations of heavy metals in addition to exposure to chemicals leaching from the particles themselves (Song et al., 2022). Furthermore, *in vitro* transmission electron microscopy studies of mitochondria in the human lung cell line BEAS-2B have revealed that PM can accumulate within mitochondria themselves, exacerbating structural damage to the cristae (Zheng et al., 2017). Microglial mitochondria may therefore be at additional risk. *In vivo*, exposure to air pollution in rodent models leads to microglial immune

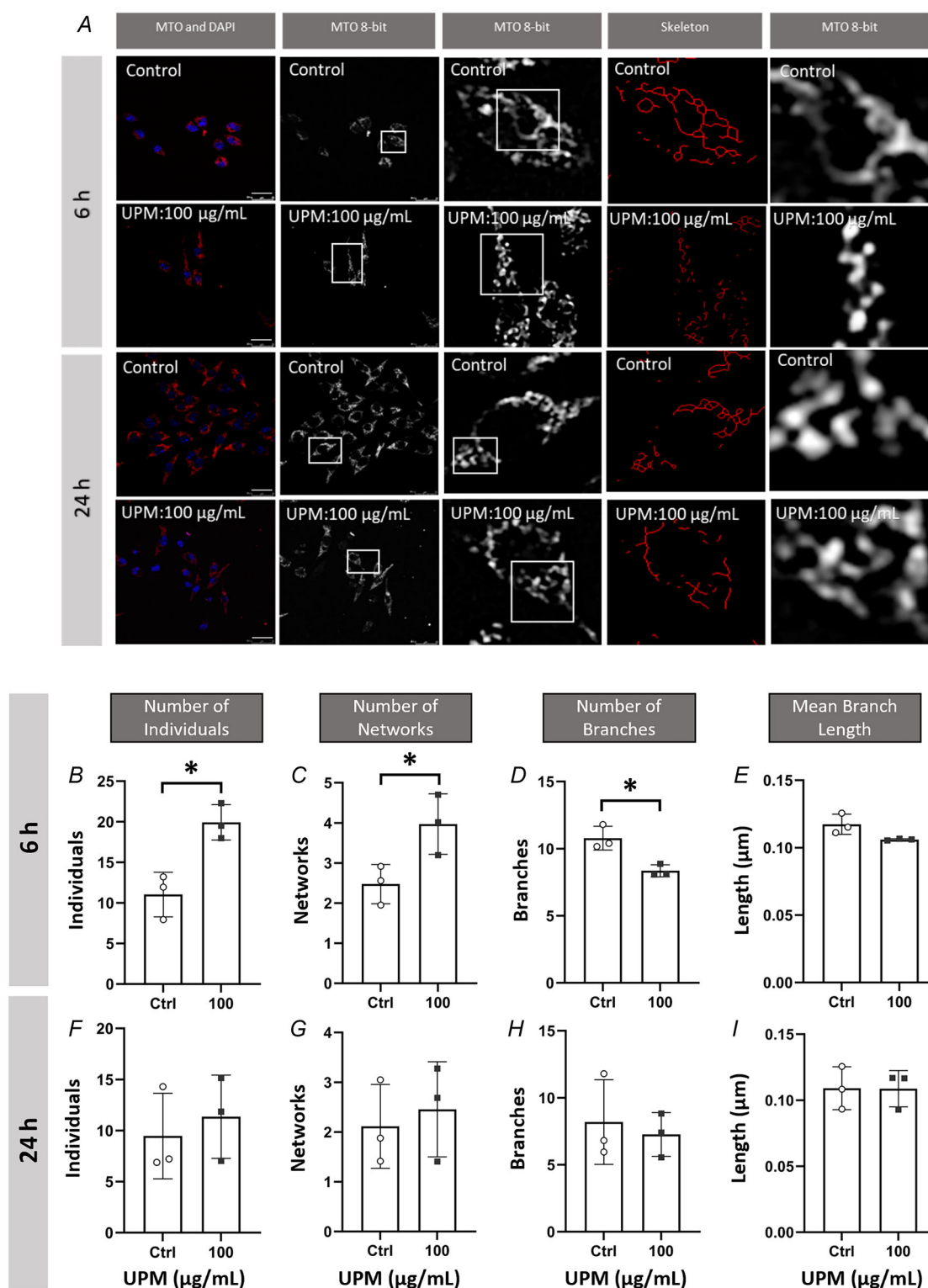


**Figure 3. Mitochondrial morphology is rapidly altered following UPM treatment**

A, BV2 cells were exposed to UPM (100 µg/mL), co-stained with Mitotracker Orange (MTO, red) and DAPI (blue), and imaged (scale bar represents 25 µm). Images were analysed using the MiNA plugin for ImageJ (Valente et al., 2017). B–D, UPM exposure (6 h, 100 µg/mL) increased the number of individuals (B, \* $P = 0.0177$ ) and networks (C, \* $P = 0.0449$ ) and decreased branch length (D, \* $P = 0.0132$ ). E–I, no change was observed in mean branch length (E) or same the metrics at 24 h after treatment (F–I). Data were analysed by a two-tailed, unpaired  $t$  test ( $N = 3$ ) and expressed as mean  $\pm$  SD. [Colour figure can be viewed at [wileyonlinelibrary.com](http://wileyonlinelibrary.com)]



activation and induction of the inflammatory response in both the adult (Costa et al., 2017) and developing brain (Bolton et al., 2017). In humans, PM in the form of black carbon was identified in cord blood and brain tissue derived from first and second trimester fetuses (Bongaerts et al., 2022; Bove et al., 2019), covering a significant period of development when microglia are first entering and proliferating in the brain (Menassa & Gomez-Nicola, 2018). The pattern and timing of microglial activation therefore become critical especially as epidemiological studies linking neurodevelopmental disorders with early life PM exposure report different outcomes depending on point of exposure (Liu et al., 2023; Rahman et al., 2022).

To investigate the consequences of UPM exposure on mitochondrial function, we performed bioenergetic

profiling by measuring oxygen consumption. Although there was variability observed in the basal respiration, markers of mitochondrial function were reduced at 6 h and increased at 24 h, resolving by 48 h to control levels. It is known that microglia can respond to myriad environmental and nutritional insults due to their capability of using a variety of metabolic substrates to maintain essential function (Nagy et al., 2018). The immediate decrease in cellular bioenergetics at 6 h followed by a rebound of mitochondrial function at 24 h may represent the time frame of the compensatory response in BV2 cells, which is complete by 48 h. The increase in mitochondrial function at 24 h is not merely as a result of the increased mitochondrial footprint (seen in the mitotracker staining, Fig. 5) as the mitochondrial

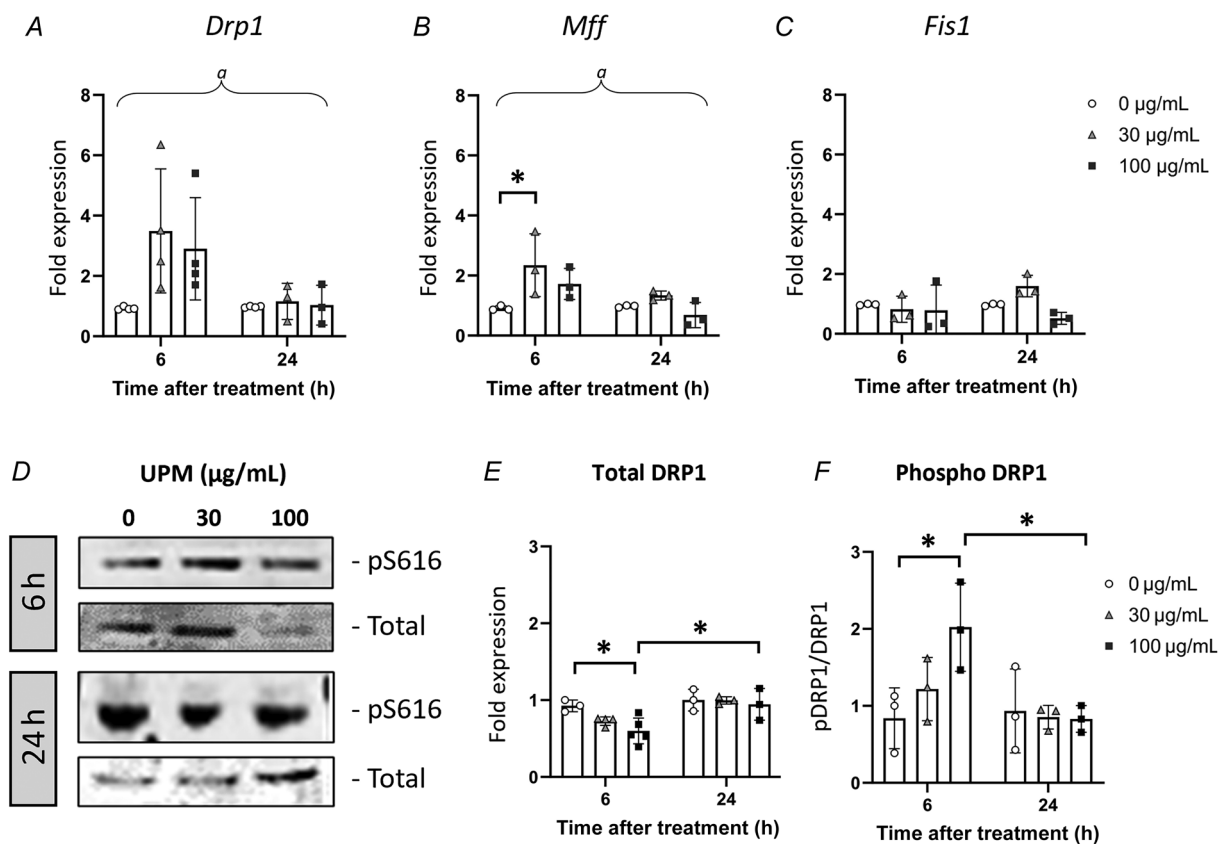


**Figure 4. Markers of mitochondrial fission alter after UPM exposure**

RNA was prepared from UPM-exposed cells and qRT-PCR was performed using primers specific for the genes shown. All values are compared against GAPDH and an experimental control. A and B, there was an increased expression of (A) *Drp1* ( $^aP = 0.0162_{[time]}$ ) and (B) *Mff* ( $^aP = 0.0181_{[time]}$ ,  $^aP = 0.0284_{[conc]}$ , 6 h 0 µg/mL vs. 30 µg/mL,  $^*P = 0.0447$ ) after 6 h of UPM exposure. C, there was no change to *Fis1* expression at 6 h nor *Drp1*, *Mff* and *Fis1* at 24 h after exposure. Data were analysed by a two-way ANOVA followed by Tukey *post hoc* test. Biological replicates are indicated on the graphs ( $N = 3$ , performed in duplicate) and expressed as mean  $\pm$  SD. D, whole-cell BV2 lysates (50 µg) were analysed by western blot for pDRP1-S616 and total DRP1 at 6 and 24 h after UPM exposure. E and F, total DRP1 (E) and phospho DRP1 (F) expression were analysed by densitometry and normalized to a total protein stain (TPS, not shown). E, total DRP1 protein was significantly decreased at 6 h (0 µg/mL vs. 100 µg/mL,  $^*P = 0.0353$ ), recovering at 24 h (6 h 100 µg/mL vs. 24 h 100 µg/mL,  $^*P = 0.0271$ ). F, phosphorylated S616-DRP1 was determined as a ratio with total DRP1 (6 h 0 µg/mL vs. 100 µg/mL,  $^*P = 0.0370$ ; 6 h 100 µg/mL vs. 24 h 100 µg/mL,  $^*P = 0.0355$ ). Densitometry data are expressed as mean  $\pm$  SD ( $N = 3$ ) and analysed by two-way ANOVA followed by Tukey *post hoc* analysis.

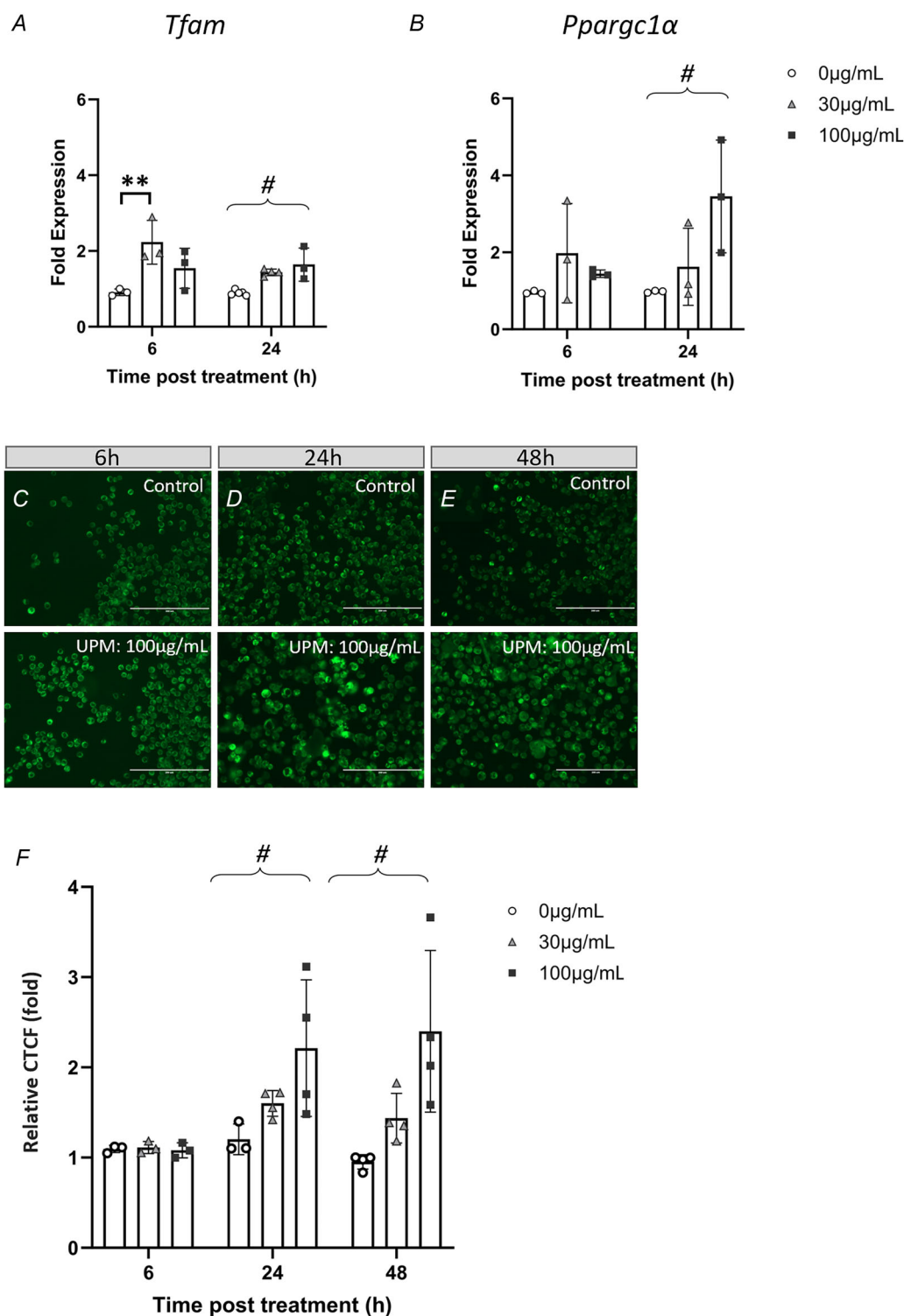


**Figure 5. Mitochondrial biogenesis may be a response to UPM exposure in BV2 cells**

A and B, qRT-PCR was performed using primers specific for *Tfam* (A, 6 h 0 μg/mL vs. 30 μg/mL,  $**P = 0.0024$ ; linear trend at 24 h,  $\#P = 0.0008$ ) and *Pparg1α* (B, 24 h, linear trend at 24 h,  $\#P = 0.0322$ ) at 6 and 24 h following treatment. Data were analysed by a two-way ANOVA followed by Tukey *post hoc* test. C–F, alterations to mitochondrial mass following UPM exposure (30–100 μg/mL) were determined with Mitotracker green uptake at 6 h (C), 24 h (D) and 48 h (E) and quantified by CTCF (F). Scale bar represents 400 μm. Data were analysed by a one-way ANOVA followed by Tukey *post hoc* test for linear trend where appropriate (linear trend at 24 h,  $\#P < 0.0001$ ; 48 h,  $\#P = 0.0003$ ). Biological replicates are as indicated on the graphs ( $N = 3–4$ ) and expressed as mean  $\pm$  SD. [Colour figure can be viewed at [wileyonlinelibrary.com](https://onlinelibrary.wiley.com)]

load is maintained at 48 h when the bioenergetic profile of UPM-exposed cells resembles that of control.

A limitation of our study is that BV2 cells experienced only a single exposure to UPM. Araujo et al. (2019) conducted a comprehensive analysis of rat brains exposed to coarse PM, PM<sub>2.5</sub> or ultrafine PM for varying durations. Notably, 1 month of exposure to PM resulted in overactivation of metabolic pathways. However, both PM<sub>2.5</sub> and ultrafine PM exposure throughout the study period ultimately led to impaired mitochondrial activity (Araujo et al., 2019). *In vitro* microglial models with repeated PM exposure will enable the longer-term cell-specific consequences of mitochondrial dysfunction to be determined.

In our study, we identified increased mitochondrial fission in response to UPM exposure, potentially via an MFF-mediated pathway. These data align with those in human vascular endothelial cells following ambient PM exposure where mitochondrial fission and pS616DRP:DRP ratio were also increased (Wang et al., 2020). However, these observations were taken at 24 h suggesting a slower response than in BV2 cells. We also saw increased mitochondrial biogenesis markers correlating with increased mitotracker green staining at 24 h suggestive of larger mitochondrial mass per cell; this is maintained at 48 h. Mitotracker green binds free thiol groups of cysteine residues and therefore is not dependent on intact membrane potential, staining all mitochondria regardless of their patency. Mitophagy and biogenesis are tightly regulated and following insult, when mitochondria become damaged, mitophagic quality control is balanced by upregulated biogenesis to restore cellular bioenergetic homeostasis (Quiles & Gustafsson, 2020). In our study, we observed increased expression of the biogenesis marker PGC1 $\alpha$  which is known to be a substrate of the metabolic sensor, AMP-activated protein kinase (AMPK) (Fan et al., 2004). As its kinase activity is rapidly triggered in response to depletion of ATP (Steinberg & Carling, 2019), which we observed at 6 h following UPM treatment, AMPK activation may be implicated in the mechanisms underpinning UPM-mediated environmental stress in microglia. Activated AMPK can also promote mitochondrial fission (a mitochondrial morphology observed in this study) via phosphorylation of MFF as well as increased mitochondrial mitophagy through phosphorylation of the autophagy regulator ULK1 (Herzig & Shaw, 2018). It remains to be determined whether AMPK-mediated mitochondrial dynamics are a target of UPM in microglial-like BV2 cells.

In summary, our collective data suggest that exposure to PM contained within urban air pollution can impact microglial bioenergetics, and microglia may mount a biogenesis-based response to combat this insult. The energy demands of the developing brain coupled with the bioenergetic stress of exposure to air pollution may

significantly increase the brain energy burden during a window of mitochondrial immaturity and reduced antioxidant capacity (Blomgren & Hagberg, 2006; Hagberg et al., 2014). As well as their reparative properties, the ability of microglia to upregulate mitochondrial biogenesis in response to environmental stress may therefore be critical at this life stage.

## References

- Araújo, J. E., Jorge, S., Santos, H. M., Chiechi, A., Galstyan, A., Lodeiro, C., Diniz, M., Kleinman, M. T., Ljubimova, J. Y., & Capelo, J. L. (2019). Proteomic changes driven by urban pollution suggest particulate matter as a deregulator of energy metabolism, mitochondrial activity, and oxidative pathways in the rat brain. *Science of the Total Environment*, **687**, 839–848.
- Arias-Pérez, R. D., Taborda, N. A., Gómez, D. M., Narvaez, J. F., Porras, J., & Hernandez, J. C. (2020). Inflammatory effects of particulate matter air pollution. *Environmental Science and Pollution Research International*, **27**(34), 42390–42404.
- Bai, K.-J., Chuang, K.-J., Chen, C.-L., Jhan, M.-K., Hsiao, T.-C., Cheng, T.-J., Chang, L.-T., Chang, T.-Y., & Chuang, H.-C. (2019). Microglial activation and inflammation caused by traffic-related particulate matter. *Chemico-Biological Interactions*, **311**, 108762.
- Bilbo, S. D., Block, C. L., Bolton, J. L., Hanamsagar, R., & Tran, P. K. (2018). Beyond infection - Maternal immune activation by environmental factors, microglial development, and relevance for autism spectrum disorders. *Experimental Neurology*, **299**, 241–251.
- Block, M. L., Wu, X., Pei, Z., Li, G., Wang, T., Qin, L., Wilson, B., Yang, J., Hong, J. S., & Veronesi, B. (2004). Nanometer size diesel exhaust particles are selectively toxic to dopaminergic neurons: The role of microglia, phagocytosis, and NADPH oxidase. *Federation of American Societies for Experimental Biology Journal*, **18**(13), 1618–1620.
- Blomgren, K., & Hagberg, H. (2006). Free radicals, mitochondria, and hypoxia-ischemia in the developing brain. *Free Radical Biology and Medicine*, **40**(3), 388–397.
- Bolton, J. L., Huff, N. C., Smith, S. H., Mason, S. N., Foster, W. M., Auten, R. L., & Bilbo, S. D. (2013). Maternal stress and effects of prenatal air pollution on offspring mental health outcomes in mice. *Environmental Health Perspectives*, **121**(9), 1075–1082.
- Bolton, J. L., Marinero, S., Hassanzadeh, T., Natesan, D., Le, D., Belliveau, C., Mason, S. N., Auten, R. L., & Bilbo, S. D. (2017). Gestational exposure to air pollution alters cortical volume, microglial morphology, and microglia-neuron interactions in a sex-specific manner. *Frontiers in Synaptic Neuroscience*, **9**, 10.
- Bongaerts, E., Lecante, L. L., Bové, H., Roeffaers, M. B. J., Ameloot, M., Fowler, P. A., & Nawrot, T. S. (2022). Maternal exposure to ambient black carbon particles and their presence in maternal and fetal circulation and organs: An analysis of two independent population-based observational studies. *The Lancet Planetary Health*, **6**(10), e804–e811.

- Bora, P., Gahurova, L., Mašek, T., Hauserova, A., Potěšil, D., Jansova, D., Susor, A., Zdráhal, Z., Ajduk, A., Pospíšek, M., & Bruce, A. W. (2021). p38-MAPK-mediated translation regulation during early blastocyst development is required for primitive endoderm differentiation in mice. *Communications Biology*, **4**(1), 788.
- Bové, H., Bongaerts, E., Slenders, E., Bijmens, E. M., Saenen, N. D., Gyselaers, W., Van Eyken, P., Plusquin, M., Roeffaers, M. B. J., Ameloot, M., & Nawrot, T. S. (2019). Ambient black carbon particles reach the fetal side of human placenta. *Nature Communications*, **10**(1), 3866.
- Chen, J., & Hoek, G. (2020). Long-term exposure to PM and all-cause and cause-specific mortality: A systematic review and meta-analysis. *Environment International*, **143**, 105974.
- Chen, X., Liu, S., Zhang, W., Wu, C., Liu, H., Zhang, F., Lu, Z., & Ding, W. (2018). Nrf2 deficiency exacerbates PM<sub>2.5</sub>-induced olfactory bulb injury. *Biochemical and Biophysical Research Communications*, **505**(4), 1154–1160.
- Chew, S., Kolosowska, N., Saveleva, L., Malm, T., & Kanninen, K. M. (2020). Impairment of mitochondrial function by particulate matter: Implications for the brain. *Neurochemistry International*, **135**, 104694.
- Costa, L. G., Cole, T. B., Coburn, J., Chang, Y. U.-C., Dao, K., & Roqué, P. J. (2017). Neurotoxicity of traffic-related air pollution. *Neurotoxicology*, **59**, 133–139.
- Costa, L. G., Cole, T. B., Dao, K., Chang, Y. U.-C., Coburn, J., & Garrick, J. M. (2020). Effects of air pollution on the nervous system and its possible role in neurodevelopmental and neurodegenerative disorders. *Pharmacology & Therapeutics*, **210**, 107523.
- Culmsee, C., Michels, S., Scheu, S., Arolt, V., Dannlowski, U., & Alferink, J. (2018). Mitochondria, microglia, and the immune system-how are they linked in affective disorders? *Frontiers in Psychiatry*, **9**, 739.
- Fan, M., Rhee, J., St-Pierre, J., Handschin, C., Puigserver, P., Lin, J., Jäeger, S., Erdjument-Bromage, H., Tempst, P., & Spiegelman, B. M. (2004). Suppression of mitochondrial respiration through recruitment of p160 myb binding protein to PGC-1 $\alpha$ : Modulation by p38 MAPK. *Genes & Development*, **18**(3), 278–289.
- Fleiss, B., Van Steenwinkel, J., Bokobza, C., K Shearer, I., Ross-Munro, E., & Gressens, P. (2021). Microglia-mediated neurodegeneration in perinatal brain injuries. *Biomolecules*, **11**(1), 99.
- Hagberg, H., Mallard, C., Rousset, C. I., & Thornton, C. (2014). Mitochondria: Hub of injury responses in the developing brain. *Lancet Neurology*, **13**(2), 217–232.
- Herzig, S., & Shaw, R. J. (2018). AMPK: Guardian of metabolism and mitochondrial homeostasis. *Nature Reviews Molecular Cell Biology*, **19**(2), 121–135.
- Jones, A., & Thornton, C. (2022). Mitochondrial dynamics in the neonatal brain - a potential target following injury? *Bioscience Reports*, **42**(3), BSR20211696.
- Karagulian, F., Belis, C. A., Dora, C. F. C., Prüss-Ustün, A. M., Bonjour, S., Adair-Rohani, H., & Amann, M. (2015). Contributions to cities' ambient particulate matter (PM): A systematic review of local source contributions at global level. *Atmospheric Environment*, **120**, 475–483.
- Kim, D., Chen, Z., Zhou, L. F., & Huang, S. X. (2018). Air pollutants and early origins of respiratory diseases. *Chronic Diseases and Translational Medicine*, **4**, 75–94.
- Kim, H., Kim, W.-H. O., Kim, Y.-Y., & Park, H.-Y. (2020). Air pollution and central nervous system disease: A review of the impact of fine particulate matter on neurological disorders. *Frontiers in Public Health*, **8**, 575330.
- Kim, R. E., Shin, C. Y., Han, S. H., & Kwon, K. J. (2020). Astaxanthin suppresses PM<sub>2.5</sub>-Induced neuroinflammation by regulating Akt phosphorylation in BV-2 microglial cells. *International Journal of Molecular Sciences*, **21**(19), 7227.
- Kleele, T., Rey, T., Winter, J., Zaganelli, S., Mahecic, D., Perreten Lambert, H., Ruberto, F. P., Nemir, M., Wai, T., Pedrazzini, T., & Manley, S. (2021). Distinct fission signatures predict mitochondrial degradation or biogenesis. *Nature*, **593**(7859), 435–439.
- Krishna, S., Arrojo E Drigo, R., Capitanio, J. S., Ramachandra, R., Ellisman, M., & Hetzer, M. W. (2021). Identification of long-lived proteins in the mitochondria reveals increased stability of the electron transport chain. *Developmental Cell*, **56**(21), 2952–2965.e9.e2959.
- Kuzawa, C. W., Chugani, H. T., Grossman, L. I., Lipovich, L., Muzik, O., Hof, P. R., Wildman, D. E., Sherwood, C. C., Leonard, W. R., & Lange, N. (2014). Metabolic costs and evolutionary implications of human brain development. *Proceedings of the National Academy of Sciences of the United States of America*, **111**(36), 13010–13015.
- Kyriakoudi, S., Drousiotou, A., & Petrou, P. P. (2021). When the balance tips: dysregulation of mitochondrial dynamics as a culprit in disease. *International Journal of Molecular Sciences*, **22**(9), 4617.
- Levesque, S., Taetzsch, T., Lull, M. E., Kodavanti, U., Stadler, K., Wagner, A., Johnson, J. O. A., Duke, L., Kodavanti, P., Surace, M. J., & Block, M. L. (2011). Diesel exhaust activates and primes microglia: Air pollution, neuroinflammation, and regulation of dopaminergic neurotoxicity. *Environmental Health Perspectives*, **119**(8), 1149–1155.
- Li, Q., Zheng, J., Xu, S., Zhang, J., Cao, Y., Qin, Z., Liu, X., & Jiang, C. (2018). The neurotoxicity induced by PM<sub>2.5</sub> might be strongly related to changes of the hippocampal tissue structure and neurotransmitter levels. *Toxicology Research (Cambridge)*, **7**(6), 1144–1152.
- Li, X., Zhang, Y., Li, B., Yang, H., Cui, J., Li, X., Zhang, X., Sun, H., Meng, Q., Wu, S., Li, S., Wang, J., Aschner, M., & Chen, R. (2020). Activation of NLRP3 in microglia exacerbates diesel exhaust particles-induced impairment in learning and memory in mice. *Environment International*, **136**, 105487.
- Liu, X., Huang, J., Song, C., Zhang, T., Liu, Y., & Yu, L. (2023). Neurodevelopmental toxicity induced by PM<sub>2.5</sub> Exposure and its possible role in Neurodegenerative and mental disorders. *Human & Experimental Toxicology*, **42**. <https://doi.org/10.1177/09603271231191436>
- Livak, K. J., & Schmittgen, T. D. (2001). Analysis of relative gene expression data using real-time quantitative PCR and the 2<sup>-ΔΔC<sub>T</sub></sup> Method. *Methods (San Diego, Calif.)*, **25**(4), 402–408.
- Mallard, C., Tremblay, M.-E., & Vexler, Z. S. (2019). Microglia and neonatal brain injury. *Neuroscience*, **405**, 68–76.



- Menassa, D. A., & Gomez-Nicola, D. (2018). Microglial dynamics during human brain development. *Frontiers in Immunology*, **9**, 1014.
- Menzies, R. A., & Gold, P. H. (1971). The turnover of mitochondria in a variety of tissues of young adult and aged rats. *Journal of Biological Chemistry*, **246**(8), 2425–2429.
- Miller, M. R. (2020). Oxidative stress and the cardiovascular effects of air pollution. *Free Radical Biology and Medicine*, **151**, 69–87.
- Misgeld, T., & Schwarz, T. L. (2017). Mitostasis in neurons: Maintaining mitochondria in an extended cellular architecture. *Neuron*, **96**(3), 651–666.
- Morris, R. H., Chabrier, G., Counsell, S. J., McGonnell, I. M., & Thornton, C. (2022). Differential effects of urban particulate matter on BV2 microglial-like and C17.2 neural stem/precursor cells. *Developmental Neuroscience*, **44**(4–5), 309–319.
- Morris, R. H., Counsell, S. J., McGonnell, I. M., & Thornton, C. (2021). Early life exposure to air pollution impacts neuronal and glial cell function leading to impaired neurodevelopment. *BioEssays*, **43**(9), e2000288.
- Nagy, A. M., Fekete, R., Horvath, G., Koncsos, G., Kriston, C., Sebestyen, A., Giricz, Z., Kornyei, Z., Madarasz, E., & Tretter, L. (2018). Versatility of microglial bioenergetic machinery under starving conditions. *Biochimica et Biophysica Acta (BBA) - Bioenergetics*, **1859**(3), 201–214.
- Navarro, A., & Boveris, A. (2004). Rat brain and liver mitochondria develop oxidative stress and lose enzymatic activities on aging. *American Journal of Physiology-Regulatory, Integrative and Comparative Physiology*, **287**(5), R1244–R1249.
- Orellano, P., Reynoso, J., Quaranta, N., Bardach, A., & Ciapponi, A. (2020). Short-term exposure to particulate matter (PM<sub>10</sub> and PM<sub>2.5</sub>), nitrogen dioxide (NO<sub>2</sub>), and ozone (O<sub>3</sub>) and all-cause and cause-specific mortality: Systematic review and meta-analysis. *Environment International*, **142**, 105876.
- Pardo, M., Qiu, X., Zimmermann, R., & Rudich, Y. (2020). Particulate matter toxicity is Nrf2 and mitochondria dependent: The roles of metals and polycyclic aromatic hydrocarbons. *Chemical Research in Toxicology*, **33**(5), 1110–1120.
- Pérez Velasco, R., & Jarosińska, D. (2022). Update of the WHO global air quality guidelines: Systematic reviews – An introduction. *Environment International*, **170**, 107556.
- Quiles, J. M., & Gustafsson, Å. B. (2020). Mitochondrial quality control and cellular proteostasis: Two sides of the same coin. *Frontiers in Physiology*, **11**, 515.
- Rahman, M. d M., Shu, Y. u-H., Chow, T., Lurmann, F. W., Yu, X., Martinez, M. P., Carter, S. A., Eckel, S. P., Chen, J.-C., Chen, Z., Levitt, P., Schwartz, J., McConnell, R., & Xiang, A. H. (2022). Prenatal exposure to air pollution and autism spectrum disorder: Sensitive windows of exposure and sex differences. *Environmental Health Perspectives*, **130**(1), 17008.
- Sama, P., Long, T. C., Hester, S., Tajuba, J., Parker, J., Chen, L.-C., & Veronesi, B. (2007). The cellular and genomic response of an immortalized microglia cell line (BV2) to concentrated ambient particulate matter. *Inhalation Toxicology*, **19**(13), 1079–1087.
- Song, J., Han, K., Wang, Y., Qu, R., Liu, Y., Wang, S., Wang, Y., An, Z., Li, J., Wu, H., & Wu, W. (2022). Microglial activation and oxidative stress in PM(2.5)-induced neurodegenerative disorders. *Antioxidants (Basel)*, **11**(8), 1482.
- Stauch, K. L., Totusek, S., Trease, A. J., Estrella, L. D., Emanuel, K., Fangmeier, A., & Fox, H. S. (2023). Longitudinal in vivo metabolic labeling reveals tissue-specific mitochondrial proteome turnover rates and proteins selectively altered by parkin deficiency. *Scientific Reports*, **13**(1), 11414.
- Steinberg, G. R., & Carling, D. (2019). AMP-activated protein kinase: The current landscape for drug development. *Nature Reviews Drug Discovery*, **18**(7), 527–551.
- Thangavel, P., Park, D., & Lee, Y. C. (2022). Recent insights into particulate matter (PM(2.5))-mediated toxicity in humans: An overview. *International Journal of Environmental Research and Public Health*, **19**(12), 7511.
- Valente, A. J., Maddalena, L. A., Robb, E. L., Moradi, F., & Stuart, J. A. (2017). A simple ImageJ macro tool for analyzing mitochondrial network morphology in mammalian cell culture. *Acta Histochemica*, **119**(3), 315–326.
- Wang, Y., Kong, L. u, Wu, T., & Tang, M. (2020). Urban particulate matter disturbs the equilibrium of mitochondrial dynamics and biogenesis in human vascular endothelial cells. *Environmental Pollution*, **264**, 114639.
- Whaley, P., Nieuwenhuijsen, M., & Burns, J. (2021). Update of the WHO global air quality guidelines: systematic reviews. *Environment International*, **142**.
- WHO. (2021). *WHO global air quality guidelines: particulate matter (PM<sub>2.5</sub> and PM<sub>10</sub>), ozone, nitrogen dioxide, sulfur dioxide and carbon monoxide. Executive summary*. World Health Organisation, Geneva.
- You, R., Ho, Y.-S., & Chang, R. C.-C. (2022). The pathogenic effects of particulate matter on neurodegeneration: A review. *Journal of Biomedical Science*, **29**(1), 15.
- Zheng, L., Liu, S., Zhuang, G., Xu, J., Liu, Q. I., Zhang, X., Deng, C., Guo, Z., Zhao, W., Liu, T., Wang, Y., Zhang, Y., Lin, J., Wang, Q., & Sui, G. (2017). Signal transductions of BEAS-2B cells in response to carcinogenic PM(2.5) exposure based on a microfluidic system. *Analytical Chemistry*, **89**(10), 5413–5421.
- Zheng, X., Wang, X., Wang, T., Zhang, H., Wu, H., Zhang, C., Yu, L. I., & Guan, Y. (2018). Gestational exposure to particulate matter 2.5 (PM<sub>2.5</sub>) leads to spatial memory dysfunction and neurodevelopmental impairment in hippocampus of mice offspring. *Frontiers in Neuroscience*, **12**, 1000.

## Additional information

### Data availability statement

The authors confirm that the data supporting the findings of this study are available within the article and available on request from the corresponding author.

### Competing interests

The authors declare there are no conflicts of interest.

## Author contributions

R.M.: Conception or design of the work; Acquisition, analysis or interpretation of data for the work; Drafting the work or revising it critically for important intellectual content; Final approval of the version to be published; Agreement to be accountable for all aspects of the work. S.C.: Conception or design of the work; Drafting the work or revising it critically for important intellectual content; Final approval of the version to be published; Agreement to be accountable for all aspects of the work. I.McG.: Conception or design of the work; Acquisition, analysis or interpretation of data for the work; Drafting the work or revising it critically for important intellectual content; Final approval of the version to be published; Agreement to be accountable for all aspects of the work. C.T.: Conception or design of the work; Acquisition, analysis or interpretation of data for the work; Drafting the work or revising it critically for important intellectual content; Final approval of the version to be published; Agreement to be accountable for all aspects of the work.

## Funding

UKRI | Biotechnology and Biological Sciences Research Council (BBSRC): Rebecca H. Morris, BB/M009513/1; UKRI | MRC | Medical Research Council: Claire Thornton, MR/T014725/1.

## Acknowledgements

This work was supported by the Biotechnology and Biological Sciences Research Council as a London Interdisciplinary Doctoral (LIDo) programme studentship to R.H.M. (BB/M009513/1) held jointly between the RVC and KCL. Work in the lab is additionally supported by the Medical Research Council (MR/T014725/1 to C.T.). We are grateful to Agilent for the extended loan of a Seahorse XF HS Mini Analyser.

## Keywords

air pollution, biogenesis, BV2, microglia, mitochondria, particulate matter

## Supporting information

Additional supporting information can be found online in the Supporting Information section at the end of the HTML view of the article. Supporting information files available:

## Peer Review History Supplementary Table 1